Macromolecules

ARTICLE

pubs.acs.org/Macromolecules

Effect of Restricted Phase Segregation and Resultant Nanostructural Heterogeneity on Glass Transition of Nonuniform Acrylic Random Copolymers

Farhad Faghihi,[†] Naser Mohammadi,*[,†] and Paul Hazendonk[‡]

[†]Loghman Fundamental Research Group, Department of Polymer Engineering and Color Technology, Amirkabir University of Technology, P.O. Box 15875-4413, Tehran, Iran

[‡]Department of Chemistry and Biochemistry, University of Lethbridge, 4401 University Dr., Lethbridge, AB T1K 3M4, Canada

ABSTRACT: The glass transition behavior of emulsion polymerized butyl acrylate (BA)−methyl methacrylate (MMA) copolymers was related to their microstructural features. Broad transition regions composed of two distinct peaks were observed in both DMA and DSC measurements of copolymers with various comonomer compositions indicating dynamic and microstructural heterogeneity. This was further investigated using 2D WISE experiment. Nanophase segregation within the copolymers was inferred from detailed analysis of their local dynamic behavior. The length scale of segregation was calculated to be 7.4 nm by ^{13}C NMR spin diffusion experiment. A modeling procedure was also developed to extract the distribution of comonomers compositions within the samples from heat flow first-derivative data. Bimodal comonomer composition distributions were extracted in accordance with their glass transition behavior.

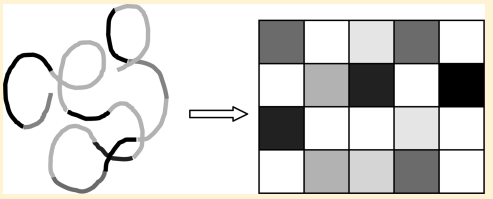

INTRODUCTION

In multicomponent polymeric systems the local segmental relaxation responsible for the glass transition is greatly affected by the detailed state of phase morphology. The glass transition characteristics of these systems which are important in applications such as mechanical wave damping[1] can thus be controlled by manipulating the fine structure of morphological heterogeneities. The scale of morphological heterogeneity can vary from local concentration fluctuations in miscible blends,[2,3] and nanophase separation in correlated random copolymers[4,5] to micro- or macrophase separation in block copolymers[6] and immiscible blends, depending on the chains microstructure and the thermodynamic affinity of components. The local nature of heterogeneity in miscible blends has led to the observation of a single broad glass transition in many studies.[2,3,7] Historically, such behavior has widely served as a criterion for miscibility. Recently, using more sensitive techniques like NMR[8] and temperature-modulated DSC[9−11] that are capable of resolving small-scale structural heterogeneities, two close-spaced yet distinct transitions have been detected in some miscible blends. This behavior was interpreted in the context of Lodge−McLeish self-concentration model which assumes higher concentration of each segment on the scale of Kuhn length due to chain connectivity.[12] According to this model, in miscible blends each monomer experiences local concentration richer in its own species in a volume $V \sim l_K^3$, where l_K, the Kuhn length, is a measure of length scale over which correlation between monomers persists along the chain.

In copolymers, the comonomers sequence distribution along the chain plays the dominant role in its phase segregation and segmental relaxation behavior. Random distribution of comonomers results in homogeneous systems with a single glass transition while ordered arrangement of comonomers into separate immiscible blocks is accompanied by appearance of distinct transitions pertaining to each component. A wide range of compositional heterogeneity at various length scales can be realized between these two extremes, through manipulation of the comonomers arrangement along the chains.[4,13−16] Mok et al.[15] investigated the phase behavior and the consequent glass transition characteristics of gradient copolymers, in which composition changed from predominantly one monomer species to a second monomer species along the copolymer backbone. Their results indicated some degree of micro- or nanophase segregation in different gradient copolymers, which among other factors was determined by chain architecture and comonomers interactions. Such phase structure was reflected as a very broad T_g consisted of overlapping transitions of domains with different compositions. More recently, they reported the correlation between the strength of nanophase segregation and the breadth of T_g in a series of weakly, moderately, and strongly segregated gradient copolymers.[16] Both their experimental results and theoretical predictions demonstrated a direct correlation between the extent of segregation, as determined by the χN parameter, and the copolymers glass transition width.

In random copolymers, statistical addition of monomers along the chains primarily promotes homogeneous microstructure. Nonetheless, difference in reactivity of comonomers and lack of thermodynamic affinity between the components can induce microstructural heterogeneity in limited length scales. Nanoscopic aggregation

Received: January 12, 2011
Revised: February 26, 2011
Published: March 11, 2011

Table 1. Recipes of Emulsion Polymerization

	samples				
	PBA	BM73	BM64	BM55	PMMA
BA (g)	14	9.8	8.4	7	
MMA (g)		4.2	5.6	7	14
water (g)	112	112	112	112	112
Triton X-100 (g)	0.42	0.42	0.42	0.42	0.42
SLS (g)	0.021	0.021	0.021	0.021	0.021
KOH (g)	0.021	0.021	0.021	0.021	0.021

was reported for the bulk films of amphiphilic random copolymer containing both hydrophilic and hydrophobic comonomers.[4] Photochemical hole-burning measurements, which are sensitive to structural relaxation behavior on the nanoscale, exhibited nanoscopic aggregation in random copolymers of methyl methacrylate with *n*-butyl methacrylate or benzyl methacrylate despite the hydrophobic nature of both monomers.[4] The existence of 20−30 nm MMA-rich domains within the random copolymers was also verified by TEM. Using 1D and 2D NMR measurements, White et al.[5] studied the dynamics and morphological heterogeneity as a function of comonomer composition in polyisobutylene/*p*-methylstyrene (PIB/PMS) correlated random copolymers. Their results indicated that while at low PMS concentration both components have similar dynamics, at higher concentration heterogeneity prevails due to the formation of PMS clusters with 3 nm domain size. Such nanophase separation was also revealed in polyanhydride random copolymers using NMR spin diffusion and SAXS experiments.[17]

In this paper a combination of solid-state NMR, DSC, and DMA measurements is used to investigate the microstructure and the glass transition behavior of butyl acrylate−methyl methacrylate random copolymers of various compositions. Broad transition regions observed in copolymer samples indicate some degree of correlation among the comonomers along the chains. Detailed analysis of dynamic heterogeneity is exploited as a promising approach to gain insight into the morphological features of the samples on the subchain scale. Furthermore, a modeling procedure is developed to obtain an estimate of the compositional distribution within the copolymers from the DSC results.

EXPERIMENTAL SECTION

Materials and Copolymer Synthesis. Methyl methacrylate and butyl acrylate monomers, sodium lauryl sulfate (ionic surfactant) and Triton X-100 (nonionic surfactant), potassium persulfate (initiator), and tertiary dodecyl mercaptan (TDM, chain transfer agent) were supplied by Merck Co. and used without further purification. Poly(methyl methacrylate) (PMMA), poly(butyl acrylate) (PBA), and methyl methacrylate/butyl acrylate copolymers with various compositions were synthesized through emulsion polymerization using predesigned recipes (Table 1). All the reagents were mixed thoroughly before adding the mixture to the reactor. The emulsion polymerization was performed within 100 cm^3 glass bottles inside a tumbling reactor at 60 °C for 24 h. The monomers conversion was found to be close to 100% using gravimetric techniques. Molecular weights of the copolymer samples were determined to be around $M_w \approx 82\,000$ g/mol by gel permeation chromatography. Test samples were prepared by latex film formation inside Petri dish at room temperature for 1 week.

DMA and DSC Measurements. Dynamic mechanical analysis (DMA) was studied over a temperature range from −90 to 110 °C with heating rate of 5 °C/min at fixed frequency of 1 Hz using a Tritec 2000 DMA instrument. The measurements were carried out in tension deformation mode on rectangular samples, around 0.6 mm in thickness, with strain amplitude less than 0.1%. This value was found to be within the linear viscoelastic region of all samples from the dynamic strain sweep experiments.

Differential scanning calorimetery was performed by TA Instruments with liquid CO_2 cooling unit under a nitrogen atmosphere. All the DSC thermograms were recorded in heating cycles from −75 to 130 °C at heating rate of 10 °C/min on the samples without prior thermal treatment. In one case, annealing was performed at 120 °C for 20 min under a nitrogen atmosphere to completely remove the thermal history. The sample was then cooled to −75 °C at a rate of 10 °C/min and subsequently heated to 120 at 10 °C/min. The heat flow data were recorded on the last heating run. At least two identically prepared samples from each copolymer were tested.

Solid-State NMR. Solution-state ^{13}C spectra were recorded on a 300 MHz Bruker spectrometer in deuterated toluene. Measurements were made at 75.5 MHz and calibrated with respect to the solvent signals. 3000 scans were accumulated with 15 s delay time between consecutive scans.

Solid-state NMR experiments were carried out on a 500 MHz wide-bore Varian Inova spectrometer using either a 2 or 4 mm Varian T-3 HFXY magic angle spinning probe. Spectra were recorded at temperatures ranging from −20 up to 45 °C at 8 kHz magic angle spinning. The 90° pulse lengths were in the range of 2.5−3.5 μs. Proton transverse relaxation times (T_2) were obtained by Hahn-echo measurement fitted to monoexponential decay. The 2D wide-line separation (WISE) spectra[18] were acquired with 128 increments and of 5000 complex data points.

The dipolar filter pulse sequence[19,20] was used in both T_1 and spin diffusion measurement. For T_1 measurement, a filter with 100 μs interpulse delay was repeated 25 times to completely suppress the spin magnetization. The recovery of the longitudinal for each signal was recorded as a function of mixing time. For proton spin diffusion measurements, the interpulse delay was set to 10 μs, and the filter was repeated five times to suppress the signals from rigid domains. After applying the filter, the remaining magnetization was alternatively stored on the $+z$ and $-z$ directions to enable T_1 correction. A sufficient number of transients was collected in order to achieve a suitable signal-to-noise ratio.

For the 2D-WISE, T_1, and spin diffusion measurements, the spectra were collected on ^{13}C after cross-polarization from ^1H. The optimum cross-polarization condition was found using a set of arrayed experiments. On the basis of these experiments, the contact time was set to 1.2 ms, the proton locking field was kept constant at 60 kHz, and the carbon locking field was ramped from 73 to 77 kHz.

RESULTS

Dynamic mechanical data of neat PMMA and BA-MMA copolymers with various compositions are shown in Figure 1. The PMMA homopolymer showed two distinct relaxations at well-separated temperatures. The relaxation at higher temperature is the main chain cooperative α transition, and the lower temperature one is the β relaxation which mainly involves rotational motion of the side chain. In comparison to the homopolymer, rather broad glass transitions are observed in copolymer samples consisting of two major overlapping peaks. The peak temperatures shifted toward higher values, and the transition region broadened with increasing the MMA content from 30 to 50 wt %. The temperature and width of transitions as determined from loss modulus curves are reported in Table 2.

DSC thermograms of the synthesized homopolymers and copolymers measured at heating rate of 10 K/min, and the corresponding heat flow first derivative curves are presented in Figure 2a,b. Analysis of derivative curves has been proven as an appropriate method of extracting quantitative data such as the

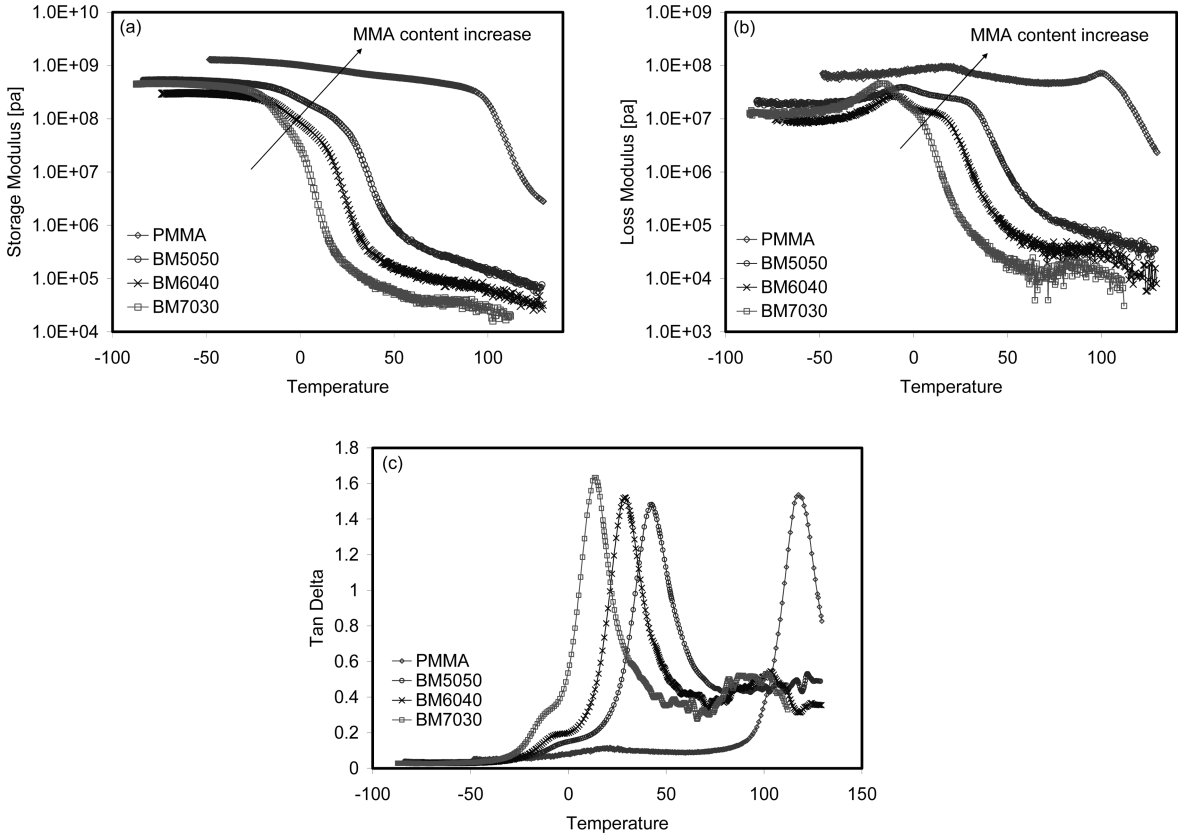

Figure 1. Dynamic mechanical behavior of PMMA and its copolymer with various compositions at 1 Hz.

Table 2. Glass Transition Characteristics of Samples

	DMA			DSC		
	T_L[a]	T_H[b]	T_g width	T_L	T_H	T_g width
PMMA		118	30		112	19
BM7030	−17.9	1	70	−31	−12	53
BM6040	−10.6	16.5	79	−24	4	64
BM5050	−6.7	23	91	−16	14	75
PBA				−51		15

[a] Lower temperature transition. [b] Higher temperature transition.

glass transition peak temperature and width from DSC curves.[9,13] This method could be specifically useful to study the transition behavior in samples with broad T_g where the heat flow changes rather weakly with temperature at glass transition. The approach for determination of T_g breadth is illustrated in Figure 2b. Similar to DMA data, copolymer samples exhibited much broader transition with double sigmoidal heat flow curves in this region. More interestingly, two distinct peaks were resolved in heat flow derivative curves for all copolymer compositions, indicating two major glass transitions in these samples. This fine structure of the main transition is in complete agreement with dynamic-mechanical measurements.

Figure 3 shows a typical solution-state NMR ^{13}C spectrum of the 60/40 butyl acrylate−methyl methacrylate copolymer recorded at room temperature. The solvent peaks were omitted from the spectrum for the sake of clarity. The side-chain carbons, specifically those belong to the BA units, have narrow peaks comparing to the main-chain carbons due to motional averaging.

An example of 2D WISE spectrum of the BM6040 sample at room temperature is presented in Figure 4. There is a noticeable difference in the line width of the components. This indicates larger average dipolar couplings experienced by MMA repeat units compared to BA units.

Since both the polymerization process and the film formation were performed in water media, copolymer particles in latex or during film formation may adopt some sort of temporary microstructure which results in the observed behavior. To investigate this possibility, heat flow curves of the BM5050 sample were recorded after annealing at 120 °C for a sufficiently long time (Figure 5). If the dynamic heterogeneity of the copolymer originates from a temporary inhomogeneous morphology, the chains should randomize upon annealing at sufficiently high temperatures. However, the transition region of the annealed sample is similar to the untreated sample within the experimental error. Therefore, heterogeneity of the copolymers is actually caused by chemical structure of the chains.

DISCUSSION

The presence of two overlapping but distinct transitions in both DMA and DSC curves reveals interesting information about the morphological features of the synthesized copolymers. It has been shown that DSC measurements are sensitive to the local environment down to the length scale of a cooperatively rearranging region (CRR) and can resolve two distinct transitions even in miscible blends.[9−11] However, conventional DMA measurements are not sensitive to such small length scales, and only a single peak appears in the dynamic mechanical spectrum of miscible blends. A single dynamic mechanical glass transition was

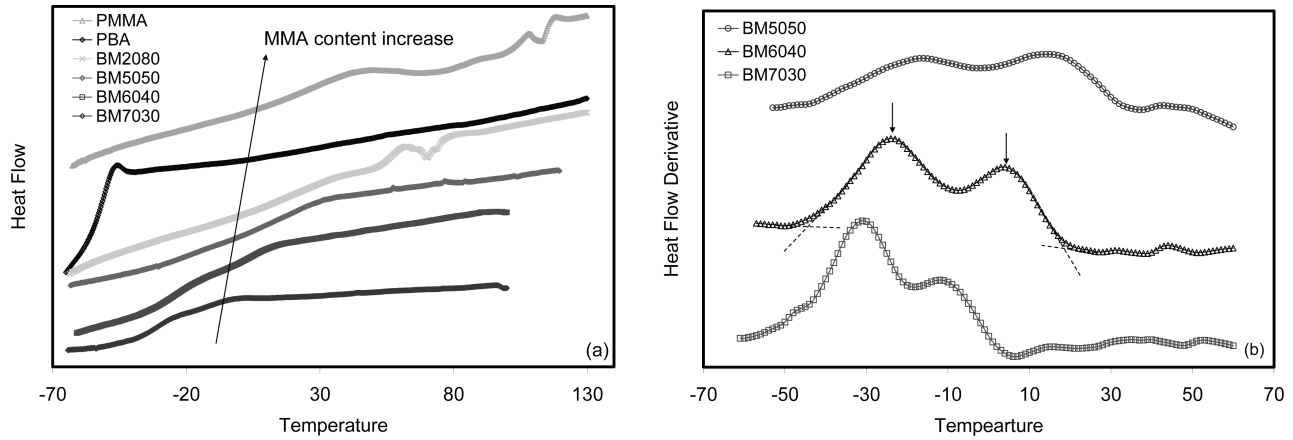

Figure 2. DSC thermograms of PMMA and PBA homopolymers and their copolymers with different compositions at heating rate of 10 °C/min (a) heat flow and (b) first-derivative curves. For copolymer curves the BA content increases from top to bottom. Determination of the onset, end point, and peak temperatures of glass transition are shown in (b).

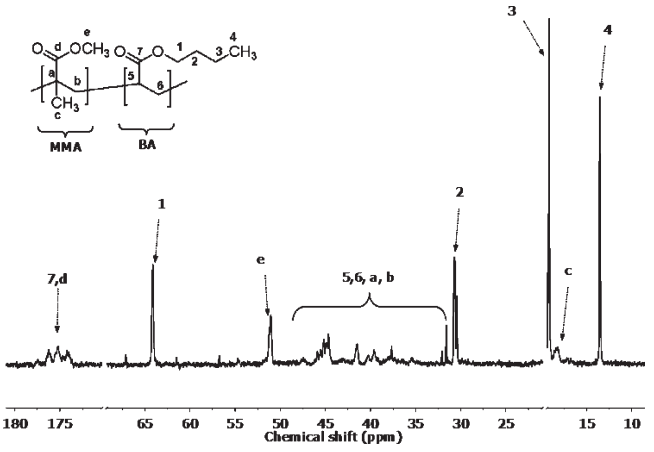

Figure 3. Solution-state ^{13}C spectrum of BM6040 sample at room temperature.

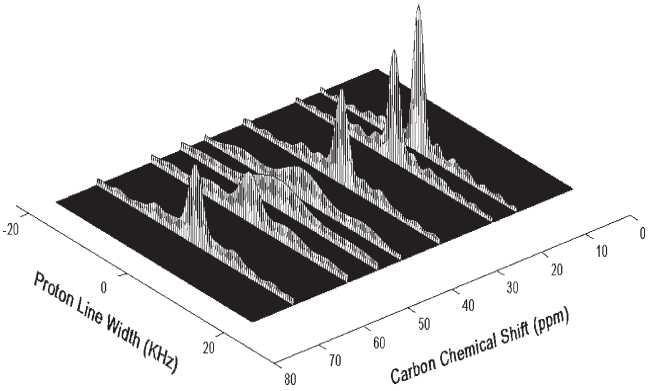

Figure 4. 2D WISE spectrum of BM6040 sample at room temperature and 8 kHz spinning speed.

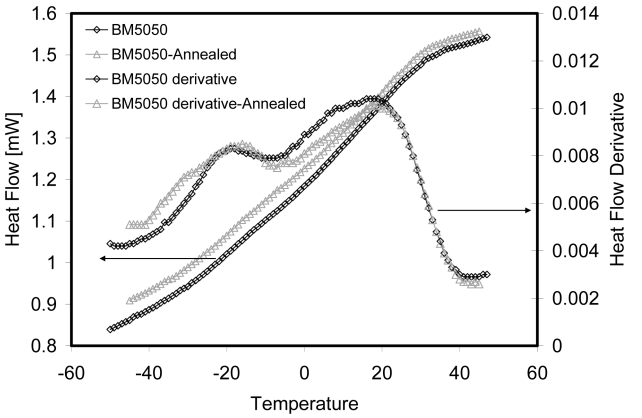

Figure 5. Comparison of the heat flow and first-derivative curves of BM5050 sample before and after annealing.

Table 3. Line Width at Half-Maximum of the Side-Chain Signals Extracted from the BM6040 WISE Spectrum at Room Temperature

signal (ppm)	14	19	32	52	65
line width (kHz)	2.65	2.87	3.35	5.63	3.75

also reported in the literature for homogeneous BA/MMA random copolymers with BA content greater than 50 wt %.[21] Therefore, two distinct transitions in calorimetric and dynamic mechanical measurements indicate some degree of phase separation at length scales larger than the local concentration fluctuation or self-concentration effect which is on the order of the Kuhn length and usually does not exceed 2 nm. On the other hand, the transitions of the copolymers under investigation are close and overlapping contrary to the two rather unchanged transitions in block copolymers with immiscible block. Thus, the amplitude of segregation is definitely smaller than that of block copolymers. In fact, the observed glass transition behavior resembled the systems with restricted phase separation such as IPNs[21,22] and gradient copolymers.[13−16]

Considering the dependences of proton line width on the local chain mobility, the disparity between the line width of the BA and MMA signals in the 2D WISE spectrum of the BM6040 sample could be related to dynamic and structural inhomogeneity. The line width of different side chain signals as extracted from WISE spectrum in Figure 4 are presented in Table 3. The OCH_3 signal of the MMA side chain has significantly broader line comparing to the CH_2 and CH_3 signals of the BA side chain. The OCH_3 line is even broader than the OCH_2 signal of the BA unit despite that

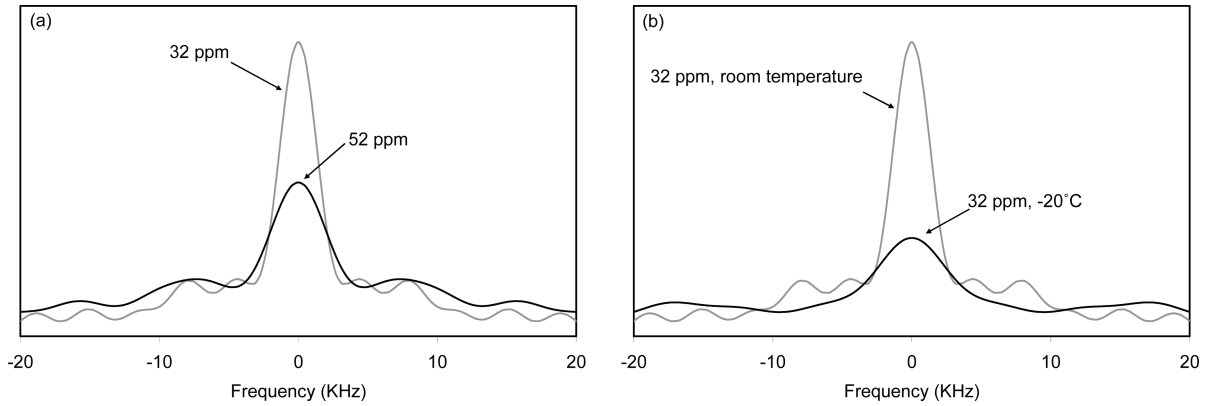

Figure 6. Selected ^{1}H line shapes from WISE spectra of BM6040 copolymer at 8 kHz spinning speed (a) BA signal at 30 ppm comparing to MMA signal at 52 ppm at room temperature (b) comparison between 30 ppm signals at room temperature (LWHM ≈ 3.35 kHz) and the same signal at −20 °C (LWHM ≈ 7.2 kHz).

the OCH_2 carbon seems to be locally more restricted. This could be related to the lower motional averaging of the dipolar interactions of the MMA units. To verify the significance of the difference in line width with respect to local mobility, it is instructive to compare the line shapes at room temperature and −20 °C. A sample comparison between the slices from WISE spectra of the BM6040 sample is shown in Figure 6. The difference between the line widths of the MMA signal at 65 ppm and the BA signal at 30 ppm is comparable to that observed for the 30 ppm line with increasing temperature from −20 °C ($T < T_g$ as determined from DMA data, Table 2) to 25 °C ($T > T_g$). This reveals the fact that on average the MMA units experience more rigid local environment with significantly slower rate of local dynamics comparing to the BA units. Therefore, in complete accordance with DMA and DSC data, 2D WISE measurements also confirm the existence of separate domains with different mobility in copolymer samples.

The restricted phase separation within the copolymer films can be assigned to the nonuniform distribution of comonomers sequences along the chain backbone. Chemical heterogeneity of the copolymer chains might be a consequence of difference in the components hydrophobicity or reactivity ratios in emulsion copolymerization reaction.[23] Irrespective of what exactly cause this heterogeneity, formation of chain sequences with large difference in BA and MMA repeat units content can increase the amplitude of local compositional heterogeneity and eventually cause segregation of these segments into BA-rich and MMA-rich domains. The close overlap of transitions in both DMA and DSC curves is an indication of restricted segregation due to the chain connectivity. It also implies that there is probably no sharp boundary between domains, and the composition changes rather gradually with some degree of randomness inherent to the copolymerization process.

The amplitude of segregation depends, among several factors, on thermodynamic affinity of comonomers and their composition. Absence of attractive interactions between MMA and BA units induces segregation if sequences of each comonomer grow sufficiently long. The sequence lengths are determined by the comonomer compositions. If the copolymer is far from symmetric composition, the probability of sufficiently long sequences from the minor component is rather negligible, and the behavior is dominated by the major component. However, the probability increases as the symmetric comonomer composition is approached. This hypothesis can be verified by comparing DSC

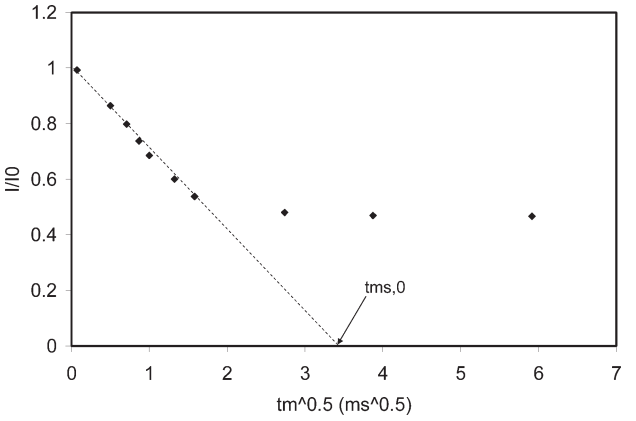

Figure 7. Spin diffusion curve of the BM5050 copolymer plotted as the normalized intensity of BA ^{13}C signal at 14 ppm versus the square root of the mixing time. The dashed line shows the initial rate approximation.

curves of copolymers with various compositions. The BM2080 heat flow curve is closely similar to that of methyl methacrylate homopolymer, except that the T_g has shifted to lower temperatures. But the breadth of glass transition increases with increasing MMA content from 30 to 50 wt %, suggesting stronger segregation (Table 2).

Length scale of the segregation domains could be determined from spin diffusion measurements. Figure 7 shows the spin diffusion curves of BM5050 sample at room temperature plotted as the normalized intensity of BA signal versus the square root of the mixing time, $\sqrt{t_m}$. At small mixing times the curve is linear to a good approximation. Therefore, the size of mobile domains (d_{mobile}) was obtained using the initial rate approximation method:[23]

$$d_{\text{mobile}} = \frac{2\varepsilon}{\sqrt{\pi}}\sqrt{D_{\text{eff}} t_{\text{m}}^{s,0}}$$

where the value $\sqrt{t_m^{s,0}}$ is shown in Figure 7, D_{eff} is the effective spin diffusion coefficient, and ε is a "dimensionality" parameter determined by the geometry. This parameter was set to 3 assuming discrete phase morphology. Moreover, half of the cross-polarization period was added to the mixing times because spin diffusion occurs during this period. The D_{eff} is related to the effective spin diffusion coefficients of rigid and mobile domains

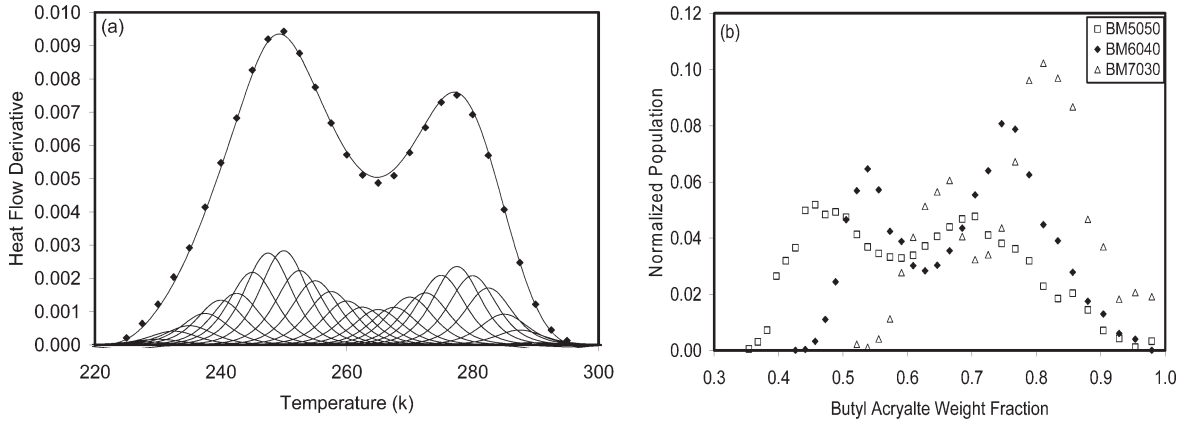

Figure 8. (a) Heat flow derivative modeling procedure for BM5050 sample. Adding up the contributions from all subunits with appropriate weighting factors gives a close fit to the experimental data. (b) Normalized comonomer distribution functions for three copolymer samples.

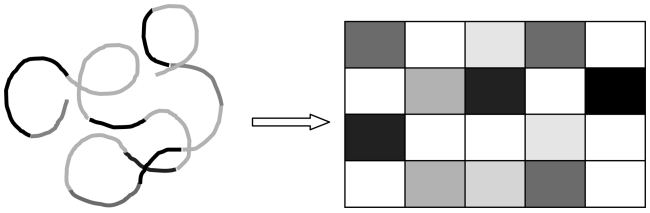

Figure 9. Schematic representation of compositional nonuniformity along the copolymer chain and the consequent nanophase-segregated structure.

by following equation:

$$\sqrt{D_{\text{eff}}} = \frac{\sqrt{D_{\text{rigid}} D_{\text{mobile}}}}{(\sqrt{D_{\text{rigid}}} + \sqrt{D_{\text{mobile}}})/2}$$

The spin diffusion coefficient is proportional to the dipolar coupling strength. Therefore, its value can be determined from the transverse relaxation rate:[20,24]

$$D(T_2^{-1}) = (8.2 \times 10^{-6} T_2^{-1.5} + 0.007)\ \text{nm}^2/\text{ms}$$
$$\text{for } 0 < T_2^{-1} < 1000\ \text{Hz}$$

$$D(T_2^{-1}) = (4.4 \times 10^{-4} T_2^{-1} + 0.26)\ \text{nm}^2/\text{ms}$$
$$\text{for } 1000 < T_2^{-1} < 3500\ \text{Hz}$$

The above equations give $D_{\text{rigid}} = 0.81\ \text{nm}^2/\text{ms}$ and $D_{\text{mobile}} = 0.12\ \text{nm}^2/\text{ms}$, which are within the range of values reported in the literature. Using these parameters, the domain size was calculated around 7.4 nm. The major source of uncertainty in determination of the domain size was the calculation of diffusion coefficients from semiexperimental equations. A more exact result could be obtained using diffusion coefficients obtained experimentally from microscopy techniques. However, the calculated length scale of separation is consistent with the transition behavior of samples in DMA and DSC curves.

According to the morphological picture obtained for the copolymers, it is possible to extract quantitative information about the comonomer composition distribution within the samples through simulation of the heat flow first-derivative curves. The nanophase-separated structure of the copolymer films can be modeled as an ensemble of homogeneous subunits; each one has its own characteristic composition and segmental relaxation behavior corresponding to its local environment. The glass transition of the whole sample is then the superposition of all the subunits transitions. This basic picture was employed to obtain the population distribution of composition within the copolymers by fitting a model to heat flow first-derivative data. Several assumptions were made for modeling:

1. The total breadth of transition was divided into m equal temperature intervals. The Fox equation was used to describe the correlation between the glass transition temperature and the composition of each subunit: $1/T_g = \phi_1/T_{g,1} + \phi_2/T_{g,2}$.
2. The heat flow derivative of a single subunit was represented by a slightly modified tanh derivative function:[12,15] $y = 1 - (\tanh((T - T_g)/w))^2$, where T_g is the glass transition peak temperature of the subunit and w determines peak width. This parameter was set to 15 based on the pure components data.
3. The intensity of the relaxation function was presumed to be proportional to the fraction of subunits that locates within each interval and appeared as a weighting factor of the relaxation function.

Employing the above assumptions, summation of weighted relaxation functions was fitted to the experimental heat flow curve, and the weighting factors were obtained as the normalized population of subunits. As is evident in Figure 8a, very close fit to the experimental data was obtained, which gave a bimodal comonomer population distribution within the samples (Figure 8b). Although the result of modeling is not accurate due to simplifying assumptions, it provides estimation of compositional profile within the correlated random copolymer samples that is certainly useful in their future applications.

CONCLUSIONS

The glass transition behavior of butyl acrylate−methyl methacrylate random copolymers was investigated by DMA, DSC, and solid-state NMR experiments. Contrary to the homogeneous random copolymers, BA−MMA copolymers exhibited broad transition regions with two distinct but overlapping peaks in both calorimetric and dynamic-mechanical measurements. 2D WISE spectra also revealed significant difference between the line width of the MMA and BA signals. This behavior was attributed to the nonuniform distribution of comonomer sequences along the copolymer chains which eventually lead to the segregation of MMA-rich from BA-rich segments into nanophase domains.

Therefore, the studied copolymers are not truly random. The extent of nonuniformity and the consequent segregation increased in copolymers as the symmetric comonomers composition was approached. The length scale of segregation was determined 7.4 nm from spin diffusion measurements. The proposed copolymer chain microstructure and the resultant nanoscale morphological heterogeneity are shown in Figure 9. A model was developed to extract quantitative information about microstructural heterogeneity from the heat flow first-derivative curves. Bimodal comonomer composition distributions were obtained for the copolymer samples in accordance with their glass transition behavior.

AUTHOR INFORMATION

Corresponding Author
*E-mail: mohamadi@aut.ac.ir.

REFERENCES

(1) Faghihi, F.; Mohammadi, N.; Haghgoo, M. *J. Polym. Sci., Part B: Polym. Phys.* **2010**, *42*, 82–88.
(2) Roland, C. M.; Ngai, K. L. *Macromolecules* **1991**, *24*, 2261–2265.
(3) Alegria, A.; Colmenero, J.; Roland, C. M.; Ngai, K. L. *Macromolecules* **1994**, *27*, 4486–4492.
(4) Kino, T.; Machida, S.; Horie, K.; Fujii, Y. *Macromolecules* **2003**, *36*, 9527–9533.
(5) White, J. L.; Dias, A. J.; Ashbaugh, J. R. . *Macromolecules* **1998**, *31*, 1880–1888.
(6) Dobrynin, A. V.; Leibler, L. *Macromolecules* **1997**, *30*, 4756–4765.
(7) Pathak, J. A.; Colby, R. H.; Kamath, S. Y.; Kumar, S. K.; Stadler, R. *Macromolecules* **1998**, *31*, 8988–8997.
(8) Haley, J. C.; Lodge, T. P.; He, Y.; Ediger, M. D.; von Meerwall, E. D.; Mijovic, J. *Macromolecules* **2003**, *36*, 6142–6151.
(9) Zhao, J.; Ediger, M. D.; Sun, Y.; Yu, L. *Macromolecules* **2009**, *42*, 6777–6783.
(10) Gaikwad, A. N.; Wood, E. R.; Ngai, T.; Lodge, T. P. *Macromolecules* **2008**, *41*, 2502–2508.
(11) Miwa, Y.; Usami, K.; Yamamoto, K.; Sakaguchi, M.; Sakai, M.; Shimada, S. *Macromolecules* **2005**, *38*, 2355–2361.
(12) Lodge, T. P.; McLeish, T. C. B. *Macromolecules* **2000**, *33*, 5278–5284.
(13) Kim, J.; Mok, M. M.; Sandoval, R. W.; Woo, D. J.; Torkelson, J. M. *Macromolecules* **2006**, *39*, 6152–6160.
(14) Karaky, K.; Péré, E.; Pouchan, C.; Desbrières, J.; Dèrail, C.; Billon, L. *Soft Matter* **2006**, *2*, 770–778.
(15) Mok, M. M.; Pujari, S.; Burghardt, W. R.; Dettmer, C. M.; Nguyen, S. T.; Ellison, C. J.; Torkelson, J. M. *Macromolecules* **2008**, *41*, 5818–5829.
(16) Mok, M. M.; Kim, J.; Wong, C. L. H.; Marrou, S. R.; Woo, D. J.; Dettmer, C. M.; Nguyen, S. T.; Ellison, C. J.; Shull, K. L.; Torkelson, J. M. *Macromolecules* **2009**, *42*, 7863–7876.
(17) Kipper, M. J.; Hou, S.; Seifert, S.; Thiyagarajan, P.; Schmidt-Rohr, K.; Narasimhan, B. *Macromolecules* **2005**, *38*, 8468–8472.
(18) Schmidt-Rohr, K.; Clause, J.; Spiess, H. W. *Macromolecules* **1992**, *25*, 3273–3277.
(19) Egger, N.; Schmidt-Rohr, K.; Blumich, B.; Domke, W. D.; Stapp, B. *J. Appl. Polym. Sci.* **1992**, *44*, 289.
(20) Mellinger, F.; Wilhelm, M.; Spiess, H. W. *Macromolecules* **1999**, *32*, 4686–4691.
(21) Espadero Berzosa, A.; Gomez Ribelles, J.; Kripotou, S.; Pissis, P. *Macromolecules* **2004**, *37*, 6472–6479.
(22) Morishima, Y.; Kobayashi, T.; Nozakura, S. *Polym. J.* **1989**, *21*, 267.
(23) Miwa, Y.; Sugino, Y.; Yamamoto, K.; Tanabe, T.; Sakaguchi, M.; Sakai, M.; Shimada, S. *Macromolecules* **2004**, *37*, 6061–6068.
(24) Neagu, C.; Puskas, J. E.; Singh, M. A.; Natansohn, A. *Macromolecules* **2000**, *33*, 5976–5981.